

FEB 22 1989

CONF-890679-1

See last page

# TWO-DIMENSIONAL PHASE CORRECTION OF SYNTHETIC APERTURE RADAR IMAGERY

Dennis C. Ghiglia and Gary A. Mastin  
Sandia National Laboratories  
Albuquerque, NM 87185

SAND--89-0411C  
DE89 007086

## Abstract

A two-dimensional synthetic aperture radar (SAR) phase correction algorithm is described as a natural extension of a one-dimensional technique developed previously. It embodies many similarities to phase gradient speckle imaging and incorporates improvements in phase estimation. Diffraction limited performance has been obtained on actual SAR imagery regardless of scene content or phase error structure. The algorithm is computationally efficient, robust, and easily implemented on a general purpose computer or special purpose hardware.

## Introduction

The two-dimensional SAR phase correction algorithm described in this summary is a natural extension to the one-dimensional (1-D) algorithm developed previously<sup>[1]</sup>. Two-dimensional (2-D) phase estimation problems abound in optics and astronomy and we anticipate that certain coherent imaging systems such as SAR or inverse SAR (ISAR) will need to confront 2-D phase correction directly, especially as performance requirements increase, operational conditions become more severe, and novel imaging and exploitation techniques are invented.

We have recently discovered that the algorithm independently developed for SAR, which has been designated as the phase gradient autofocus (PGA) algorithm, has its counterpart in optics. The phase gradient algorithm for speckle imaging<sup>[2-4]</sup> (an alternative to the Knox-Thompson method<sup>[5,6]</sup>) is completely analogous to the SAR phase correction technique with two noteable distinctions. First, SAR imaging offers the advantage of storing the complex imagery, thus allowing phase correction iterations. Second, the phase error is the redundant information in SAR imagery. This is in direct contrast to the imaged scene supplying the redundancy in multiple speckle images. These distinctions will be addressed more thoroughly in the discussion of algorithm implementation.

The phase gradient algorithm applied to SAR is a linear unbiased minimum variance (LUMV) estimator<sup>[7]</sup>, thus perhaps helping to explain the algorithm's robustness. It should be noted that any algorithm requiring a least squares phase estimate from phase gradients

MASTER

## **DISCLAIMER**

**This report was prepared as an account of work sponsored by an agency of the United States Government. Neither the United States Government nor any agency thereof, nor any of their employees, makes any warranty, express or implied, or assumes any legal liability or responsibility for the accuracy, completeness, or usefulness of any information, apparatus, product, or process disclosed, or represents that its use would not infringe privately owned rights. Reference herein to any specific commercial product, process, or service by trade name, trademark, manufacturer, or otherwise does not necessarily constitute or imply its endorsement, recommendation, or favoring by the United States Government or any agency thereof. The views and opinions of authors expressed herein do not necessarily state or reflect those of the United States Government or any agency thereof.**

---

## **DISCLAIMER**

**Portions of this document may be illegible in electronic image products. Images are produced from the best available original document.**

or phase differences could perhaps benefit from the phase reconstruction method described in [8] and implemented here.

A SAR system transmits and receives coherent broadband signals which may be subjected to perturbations due to platform velocity errors in azimuth coupled with other perturbations such as atmospheric turbulence. The received data are stored, combined, and processed to synthesize a large aperture, which is then focused to produce a high-resolution terrain image<sup>[9–11]</sup>. These processing steps are similar, in many respects, to data gathering and image formation in tomography<sup>[12]</sup>, aperture synthesis radio astronomy<sup>[13]</sup>, and other fields. We have adopted a nomenclature common to aperture synthesis radio astronomy where data gathered in the Fourier domain is denoted by an uppercase letter and dimensional variables  $u$  and  $v$ . This nomenclature is, however, different from that used in the 1-D SAR algorithm<sup>[1]</sup>.

In this summary,  $g(x, y)$  shall refer to the complex image and  $G(u, v)$  shall refer to the complex phase history.  $g(x, y)$  and  $G(u, v)$  are related through a 2-D Fourier transform,  $G(u, v) = \mathcal{F}\{g(x, y)\}$ . The complex image,  $g(x, y)$ , is composed of the true, unperturbed scene,  $f(x, y)$ , convolved with the point spread function (PSF) due to the phase error,  $g(x, y) = f(x, y) * h(x, y)$ , where  $\mathcal{F}\{h(x, y)\} = e^{j\phi(u, v)_\epsilon}$  and  $\phi(u, v)_\epsilon$  is the 2-D phase error.

If, for simplicity, we assume that the unperturbed scene,  $f(x, y)$ , contains a sum of point-like scatterers, then  $g(x, y)$  can be written as,

$$g(x, y) = \sum_{k,l} a_{k,l} s(x - x_k, y - y_l) * h(x, y)$$

where  $a_{k,l}$  is the complex amplitude of a particular scatterer, and  $s(x, y)$  is the system response function. Thus, in the phase history domain, the perturbed phase history due to a particular scatterer,  $n$ , can be written as,

$$G(u, v) = |G(u, v)_n| e^{j[\phi(u, v)_n + \phi(u, v)_\epsilon]}$$

where  $|G(u, v)_n|$  and  $\phi(u, v)_n$  are the magnitude and phase over the aperture induced by scatterer  $n$ . Note that  $\phi(u, v)_\epsilon$  is the phase error common to all scatterers and, hence, independent of  $n$ .

We obtain a LUMV estimate for  $\phi(u, v)_\epsilon$ , denoted  $\hat{\phi}(u, v)_\epsilon$ , by appropriate processing of the  $G(u, v)_n$ . A particular method for obtaining the  $G(u, v)_n$  from a single image,  $g(x, y)$ , will be discussed later. The  $u$  and  $v$  components of the LUMV estimate for the phase gradient (containing the gradient of the redundant phase error) is computed from the following sums once the  $G(u, v)_n$  are obtained.

$$\dot{\phi}_u(u, v) = \frac{\sum_n \text{Im}\{\dot{G}_u(u, v)_n G_u^*(u, v)_n\}}{\sum_n |G_u(u, v)_n|^2} = \dot{\phi}_u(u, v)_\epsilon + \frac{\sum_n |G_u(u, v)_n|^2 \dot{\phi}_u(u, v)_n}{\sum_n |G_u(u, v)_n|^2} \quad (1)$$

and

$$\dot{\phi}_v(u, v) = \frac{\sum_n \text{Im}\{\dot{G}_v(u, v)_n G_v^*(u, v)_n\}}{\sum_n |G_v(u, v)_n|^2} = \dot{\phi}_v(u, v)_\epsilon + \frac{\sum_n |G_v(u, v)_n|^2 \dot{\phi}_v(u, v)_n}{\sum_n |G_v(u, v)_n|^2}$$

Thus, the LUMV phase gradient estimate yields the phase error gradient plus a residual term dependent upon scene content. Iterations drive the algorithm toward convergence.

## Implementation

The implementation of the 2-D SAR phase correction algorithm, while straightforward, highlights a significant difference between SAR phase correction and speckle imaging. In SAR phase correction, we obtain the equivalent of multiple speckle images by subdividing the perturbed complex image,  $g(x, y)$ , and processing an ensemble of  $n$  grid cells to extract the phase error responsible for image misfocus. The phase error (or equivalently the PSF) is the redundant information in each grid cell. It is removed from the SAR phase history to focus the image. In speckle imaging, the scene of interest is the redundant information present in each speckle frame. The recovered phase is the phase of the scene.

With these distinctions in mind, we now summarize the basic restoration algorithm. First, the complex image,  $g(x, y)$ , is subdivided into a set of  $n$  grid cells, each grid cell,  $g(x, y)_n$ , assuming a role similar to that of an individual speckle frame in the optical phase gradient technique. Second, the greatest magnitude pixel in each grid cell becomes the center of that cell's revised boundary. Third, the running sums in the left-most fractions of equations (1) are computed for the ensemble of  $n$  grid cell subimages. Fourth, the phase gradient components in the  $u$ - and  $v$ -dimensions,  $\phi_u(u, v)$  and  $\phi_v(u, v)$ , are computed. Fifth, the estimated phase error,  $\hat{\phi}(u, v)_\epsilon$ , is computed from the phase gradients with a fast Poisson solver<sup>[8]</sup>. Finally, the estimated phase error is removed from the phase history,  $G(u, v)$ , an improved complex image,  $g(x, y)$ , is created, and the entire process is repeated until the rms phase being computed converges or drops below some threshold.

Figure 1 shows a processed example. The 2-D phase error removed from the image was added to the unperturbed phase history prior to processing with our algorithm.

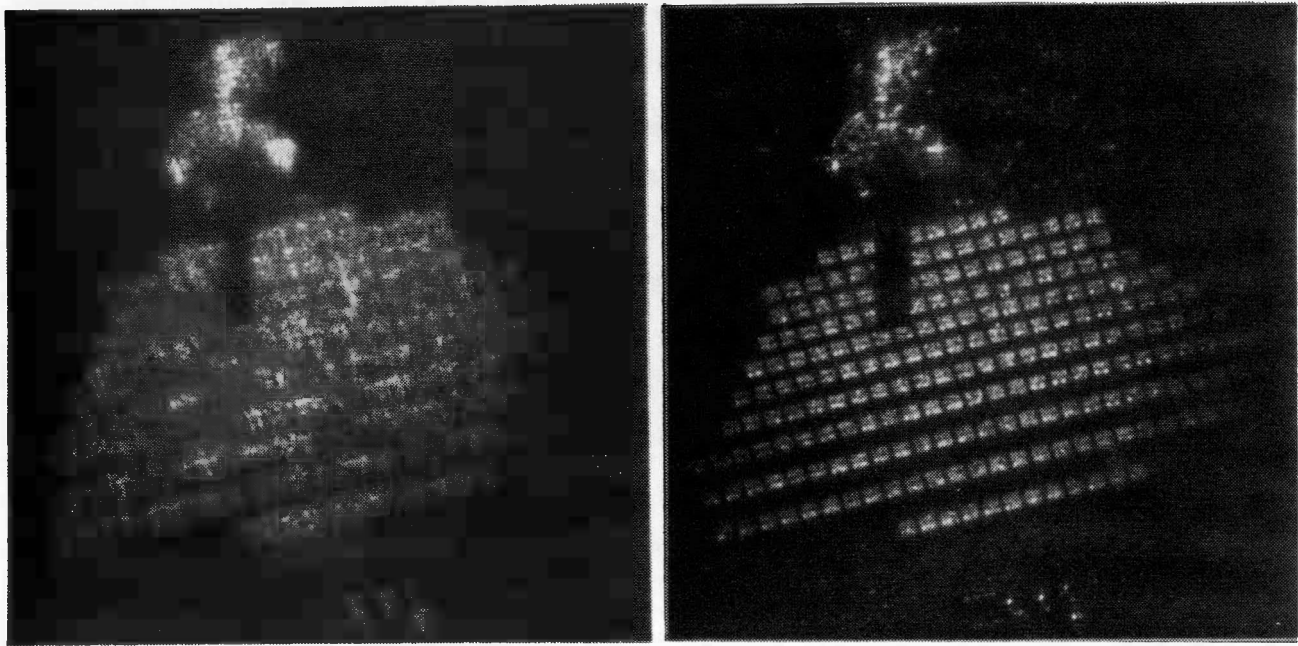


Figure 1. a) A SAR image of the Solar Thermal Test Facility at Sandia National Laboratories-Albuquerque with a 2-D phase error applied, and b) after 10 iterations of the PGA algorithm.

## Summary and Conclusions

We have highlighted the 2-D SAR phase correction algorithm as the natural extension to the previously developed 1-D algorithm. We have alluded to its similarity with the phase gradient method in speckle imaging and pointed out particular differences. We feel that the robustness of the algorithm stems from the fact that it embodies a LUMV estimator for the phase gradient. A direct (non iterative) method for estimating the phase from the phase gradient was implemented in the algorithm based on the work described in [8]. The examples of phase distorted/corrected SAR imagery indicate the algorithm's potential in the correction of arbitrary errors from atmospherics or complicated transmitter/scatterer relative motions.

We hope this presentation will help bridge a gap between the optics and radar imaging communities by highlighting some common problems and practical solutions. It is fascinating and exciting to find connections between diverse disciplines and it has ~~perked~~  our interest sufficiently so that we feel compelled to look on the "other side of the fence" a little more often.

## Acknowledgements

The authors wish to thank their colleagues P. H. Eichel, C. V. Jakowatz, Jr., and L. A. Romero for their continuing contributions. This research was performed at Sandia National Laboratories, Albuquerque, NM, for the U.S. Department of Energy under contract number DE-AC04-76DP00789.

## References

1. P. H. Eichel, D. C. Ghiglia, and C. V. Jakowatz, Jr., *Optics Lett.* **14**, 1 (1989).
2. G. J. M. Aitken, R. Johnson, and R. Houtman, *Optics Commun.* **56**, 379 (1985).
3. G. J. M. Aitken and R. Johnson, *Appl. Optics* **26**, 4246 (1987).
4. R. Johnson and G. J. M. Aitken, *J. Opt. Soc. Am. A* **6**, 56 (1989).
5. K. Knox, in *Digest of International Optical Computing Conference* (Institute of Electrical and Electronics Engineers, New York, 1975). pp. 94-97.
6. K. T. Knox and B. J. Thompson, *Astrophys. J.* **193**, L45 (1974).
7. P. H. Eichel and C. V. Jakowatz, Jr., (Submitted to *Optics Lett.*)
8. D. C. Ghiglia and L. A. Romero, (submitted to *Optics Lett.*)
9. W. M. Brown and L. J. Porcello, *IEEE Spectrum* **6**, 111 (1962).
10. D. A. Ausherman, A. Kozma, J. L. Walker, H. M. Jones, and E. C. Poggio, *IEEE Trans. Aerosp. Electron. Syst. AES-20*, 323 (1984).
11. R. O. Harger, *Synthetic Aperture Radar Systems: Theory and Design* (Academic, New York, 1970).
12. D. C. Munson, Jr., J. D. O'Brien, and W. K. Jenkins, *Proc. IEEE* **71**, 987 (1983).
13. A. R. Thompson, J. M. Moran, and G. W. Swenson, Jr., *Interferometry and Synthesis in Radio Astronomy* (Wiley, New York, 1986).